THE ASTROPHYSICAL JOURNAL, 302:296–305, 1986 March 1

THE JET OF PKS 0521−36: AN AGING COUNTERPART OF M87?

WILLIAM C. KEEL[1]
Kitt Peak National Observatory, National Optical Astronomy Observatories[2]
Received 1984 October 10; accepted 1985 August 30

ABSTRACT

Imaging photometry and VLA mapping at 2 and 6 cm have been used to study the structure and spectral energy distribution of the jet in PKS 0521−36. The jet exhibits a strong knot (1.6 kpc from the nucleus) which is resolved at 2 cm and elongated perpendicular to the jet, in a manner suggesting an internal shock. The optical continuum has a spectral index -2.0 ± 0.3, with a mean radio-to-optical index of 0.76; this steepens by 0.07 between the inner and outer parts of the jet. A spectral break frequency ~ 3 times lower than what is seen in M87 is inferred. The radio data suggest that this difference is mostly due to a lower average magnetic field in PKS 0521−36, and that the electron energy distributions in both objects extend to $\gamma \approx 10^6$.

A strong radio hot spot appears opposite the jet. It is resolved at 2 cm (characteristic dimension ~ 0.5 kpc) and has complex associated structure in both intensity and polarization. Absence of a detected counterjet suggests either a gross asymmetry in physical conditions within the galaxy (if nuclear ejection is symmetric) or a recent change of direction (for an intrinsically one-sided jet). PKS 0521−36 shares several features with M87; comparison of the galactic environments and jet morphologies is presented. Similar location of prominent knots in both suggests either that the jets respond to pressure of the galaxies' own interstellar media, or that PKS 0521−36 contains a cooling flow despite the absence of a rich cluster.

Subject headings: galaxies: individual — galaxies: jets — interferometry — radio sources: galaxies

I. INTRODUCTION

Properties of jets in active galaxies are increasingly seen as possible clues to the central energy sources and flow collimation mechanisms. The few jets directly detected optically are of special importance in extending the frequency range (electron energy range, for synchrotron-emitting jets) measured by a factor of 10^4, and in probing the role of any emission-line gas ($\sim 10^4$ K) in or near the jets.

The elliptical radio galaxy PKS 0521−36 has been studied extensively by Danziger *et al.* (1979, 1983*b*). They note the presence of an optical jet on a deep red plate and present spectra of the (variable) nucleus taken in a high state. Sol (1983) has presented preliminary results from CCD imaging and noted possible similarities with the jet of M87.

As part of a more general survey of optical jets, new imaging, spectroscopic, and radio data have been obtained for PKS 0521−36. In comparison with the well-observed case of M87, important similarities and differences have been found.

II. OBSERVATIONS

a) Optical Images

PKS 0521−36 was observed with a 320 × 512 pixel RCA CCD at the prime focus of the CTIO 4 m telescope. The image scale is 0".60 per pixel; seeing was 1".5 FWHM. Series of short exposures, to avoid saturation at the nucleus, were taken through *B* (total integration 10 minutes) and *V* (8 minutes) filters plus an interference filter with 75 Å FWHM centered at 6975 Å (including Hα and [N II] at the galaxy's redshift; total integration 16 minutes). The photometric scale was set through observation of Graham (1982) standard stars. The Hα filter has a measured transmission peak of 6975 Å, but this is shifted shortward in the strongly convergent f/2.7 beam at the prime focus; Hα is observed at 6924 Å in PKS 0521−36. Experience suggested that a shift of ~ 50 Å would occur in the mean filter wavelength; this was borne out through observations of objects with strong emission at known redshifts. While the weighting across the field is somewhat complex, Hα at the field center clearly would have been included in the passband.

Interference fringes appeared in the *V* band and λ6975 images; a standard library fringe frame was used to correct the *V* image for the effect of λ5577 night-sky emission.

Synthetic aperture photometry was performed to give integrated magnitudes and colors, both raw and (with the help of the nuclear spectrum described below) corrected for the nonthermal continuum of the nucleus. These appear in Table 1, along with other relevant data.

Further image processing was applied to produce total intensity and morphological data at *B* and *V* for the jet alone (it was only marginally detected at 6975 Å). To isolate images of the jet, the galaxy image in each passband was rotated by 180° and subtracted after an appropriate zero-point shift in each coordinate. The shifts were iteratively improved by reducing the amplitude of the residuals at the center; centering accurate to 0.1 pixel or better is necessary because the background light gradient near the nucleus is very strong. The original and jet-only *V*-band images are shown in Figure 1 (Plate 8). The *B* images are similar, except for slightly higher contrast of the jet above galaxy background. There is no evidence for $B-V$ color gradients along the jet proper ($\lesssim 5\%$ along the jet); it is also unresolved in width all along its length. A discrete knot is visible off the jet tip; it is distinctly red ($B-V > 1.5$) and may not be emission from the jet itself (§ III*c*). The reduced total jet magnitudes appear in Table 1. At $B-V = 0.65$, the jet is blue compared to the galaxy but not by comparison with such synchrotron ensembles as the M87 jet, whose spectral index of −0.9 in the optical (Keel 1984) gives

[1] Visiting astronomer, Cerro Tololo Inter-American Observatory, National Optical Astronomy Observatories.[2]

[2] Operated by the Association of Universities for Research in Astronomy, Inc., under contract with the National Science Foundation.

1986ApJ...302..296K

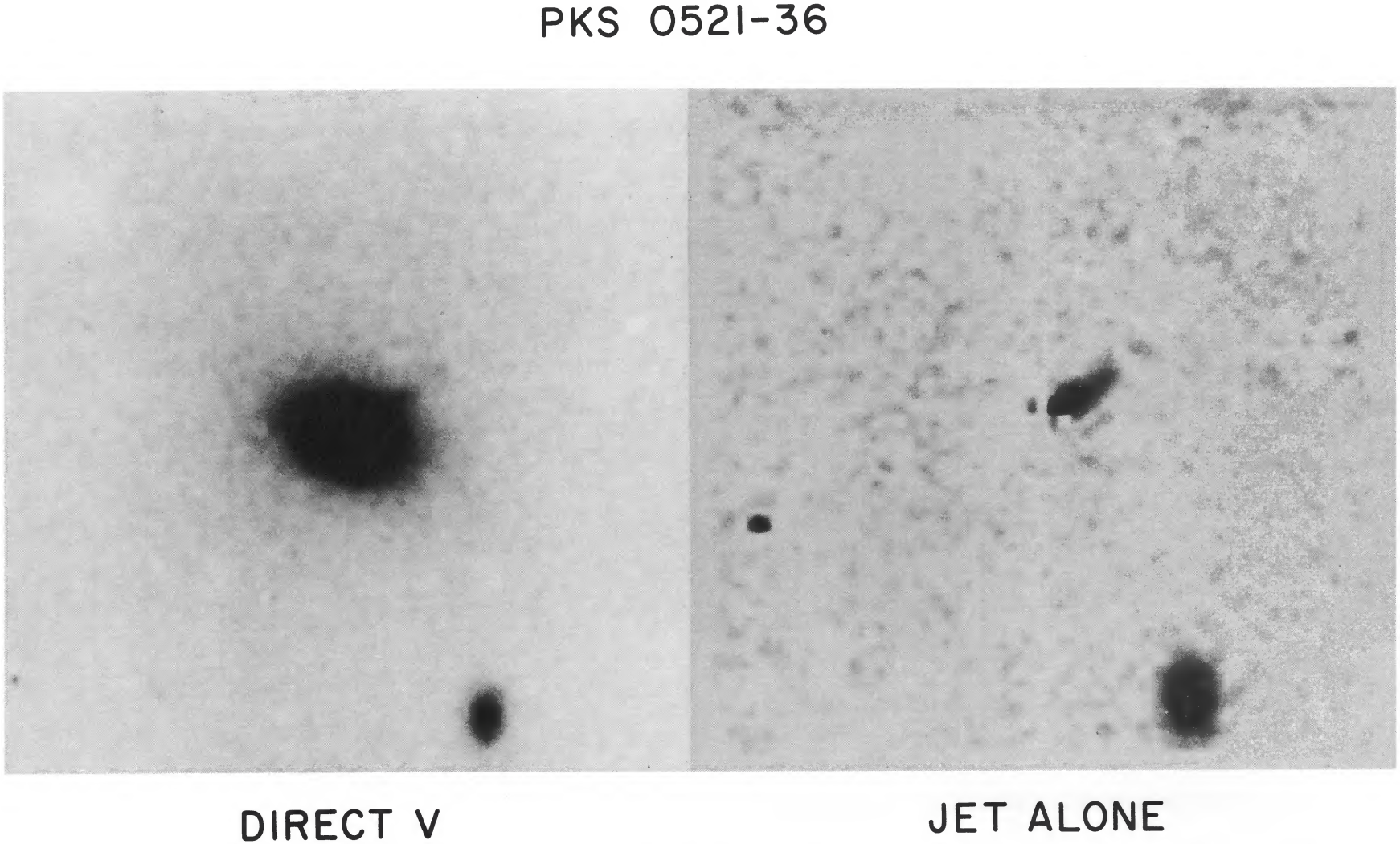

FIG. 1.—CCD images of PKS 0521 − 36 in the *V* passband. (*Left*) The reduced galaxy image. (*right*) The jet alone after subtraction of an inverted version of the galaxy image. North is at the top; the field is 60″ on a side.

KEEL (*see* page 296)

TABLE 1

CCD PHOTOMETRY OF PKS 0521−36

A.

Aperture	V	$B-V$
4.1	15.55	0.83
5.3	15.33	0.83
6.5	15.22	0.83
8.9	15.05	0.86
12.4	14.92	0.87
20.7	14.75	0.89
28.9	14.65	0.89
38.3	14.57	0.90

B.

Object	V	$B-V$
Total (extrapolated)	14.35	0.90
Nuclear nonthermal continuum	16.20	0.51
Galaxy without nonthermal	14.60	0.95
Jet alone	19.51	0.65
Knot off jet tip	22.84	...

$B-V = 0.31$, following the transformations given by Sandage (1966).

These data give a jet position angle of 302° ± 2°, in agreement with the 305° reported by Danziger *et al.* (1979).

b) Spectrophotometry

A long-slit spectrum of PKS 0521−36 was obtained on 1983 October 2 with the 40 mm SIT Vidicon on the Ritchey-Chrétien spectrograph on the CTIO 4 m telescope, covering the range 4100–7200 Å at 6 Å resolution. The slit was set to P.A. 305°, including the jet. A form of beam-pulling along the slit prevented extraction of a jet spectrum; the only conclusion possible for it is that no strong emission lines are present. A usable spectrum of the nucleus, covering an area 2″ × 5″, was extracted and flux-calibrated by reference to the standard star LDS 749B. The total exposure was 26 minutes, broken into segments of 5–7 minutes to avoid saturation or excessive beam-bending. A bias frame taken immediately beforehand was subtracted to reduce the tube's fixed-pattern background. The data were corrected for distortion along the slit and put on a linear wavelength scale with the RV package of the KPNO IPPS. Finally, the spectrum of a nearby area of blank sky from the same exposure was extracted, smoothed, and subtracted from the nuclear spectrum to reduce the effects of temporal drifts of low spatial frequency present in the detector. The reduced spectrum appears photometrically useful over the range 4500–6200 Å; an empirical correction was applied redward of this to compensate for second-order light from the very blue standard star, based on observation of elliptical galaxies with normal energy distributions.

The nuclear spectrum is shown in Figure 2. Normal features of an old stellar population are visible, diluted by the nonthermal continuum of the active nucleus. Also seen are narrow emission lines of intermediate ionization and the broad component of Hα, which appears to have been increasing in strength (Ulrich 1981). Decomposition of the nuclear spectrum is of interest, both for comparison with previous data and

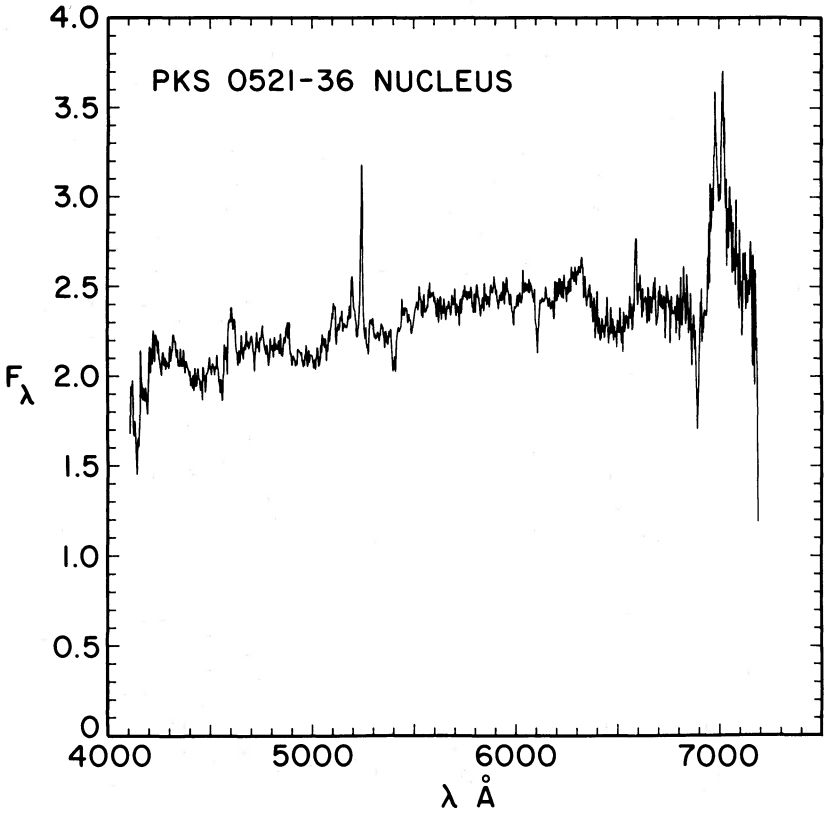

FIG. 2.—The nuclear spectrum of PKS 0521−36 as observed on 1983 October 2 with the SIT Vidicon spectrometer on the CTIO 4 m telescope. An area 2″ × 5″ was summed along the slit. The scale is in relative flux per unit wavelength. Note the prominent stellar absorption features and the broad component at Hα; the noise increases to the red because a blue-blazed grating was used.

TABLE 2

RELATIVE NUCLEAR EMISSION-LINE FLUXES IN PKS 0521−36

Line	Intensity
Hβ narrow	43
[O III] λ4959	53
[O III] λ5007	151
[N I] λ5199	16
He I λ5876 (broad)	207
[O I] λ6300	60
Hα narrow	100
Hα broad	999
[N II] λ6583	148
Estimated error, narrow lines	7

because the nonthermal component is highly variable (and is frequently called a BL Lac object for this reason).

The contribution of the stellar component to the nuclear spectrum was evaluated by using a similarly obtained spectrum of the elliptical galaxy NGC 7144, suitably scaled in velocity space. The intensity scaling for subtraction was varied until the minimum residuals in strong absorption features (Mg H, Na D) were obtained. This procedure indicated that starlight contributed 45% of the light at V in the spectroscopic aperture (area 10 arcsec^2). Danziger *et al.* (1979) found 20% in a $2'' \times 4''$ arcsec aperture; it appears safe to deduce that the nonstellar continuum was about half as bright in 1983 October as at the earlier epoch (1975). It seems to have been nearly as faint when observed by Danziger *et al.* (1983*a*) with *IUE* in mid–1980.

The slope of the nonthermal continuum remaining after starlight subtraction is $\alpha = -1.7$, where $F_\nu \propto \nu^\alpha$; the estimated error is ± 0.1 in α. This continues the trend of spectral steepening with decreasing brightness shown by the earlier data (Danziger *et al.* 1983*b*). This behavior is not unusual among BL Lac objects and violently variable QSOs.

Measures of the remaining spectral component, the emission lines, are given in Table 2. Agreement with the measures by Danziger *et al.* (1979) is generally good, except that the [O III] λ5007/λ4959 ratio in the present data is within the errors of its emitted value, fixed by atomic parameters. There is thus no evidence of an additional emission-line system displaced in redshift, previously suspected from measures of the [O III] ratio. The ionization level of the nuclear gas is midway between those typical of LINERs (Heckman 1980) and narrow-line radio galaxies (those with strong emission; Koski 1978).

The environment of PKS 0521−36 is of interest; while it is clearly not situated in an aggregate comparable to the Virgo Cluster, several galaxies appear within ~10′ on the sky whose magnitudes suggest that they might form a group at the approximate redshift of PKS 0521−36. The brightest such galaxy, an elliptical with $B \approx 16$ located at (1950) $05^h20^m46^s.2$, $-36°32'31''$, was observed with the image-dissector scanner at the University of Minnesota–University of California, San Diego 1.5 m reflector on Mount Lemmon. From Mg I + Mg H and Na D features, a redshift of $z = 0.058 \pm 0.002$ was measured, within the errors the same as that of 0521−36 itself (at $z = 0.055$). Several spirals in the vicinity were attempted but too faint to measure; the presence of a pair of giant ellipticals and a projected separation of ~400 kpc is consistent with the existence of a sparse group here.

[3] The Very Large Array is a facility of the National Radio Astronomy Observatory, which is operated by Associated Universities, Inc., under contract with the National Science Foundation.

c) *Radio Mapping*

The large-scale structure of PKS 0521−36 was mapped with the VLA[3] in its standard B configuration at 6 cm on 1984 January 21 (UT). The total integration time was 40 minutes, begun slightly after meridian passage. The nearby calibrator 0528−25 was observed before, midway through, and following the scans of 0521−36.

The dynamic range of the resulting map could be increased by the self-calibration procedure of Schwab (1980). Two such iterations were performed to reduce the effects of time-dependent phase errors; the second iteration was performed to see whether any improvement in the results due to a better initial map could be produced, but little change was apparent. For a source of this strength, it was possible to use a slightly less elliptical beam ($2'' \times 4''$) in restoring the clean map than would be generated by a Gaussian fit to the instrumental response of the standard B array at such southerly declinations; no spurious features seem to have been introduced thereby, and comparison with the optical images is somewhat eased.

A gray-scale representation of the final map is shown as Figure 3 (Plate 9). The intensity mapping employed emphasizes the faint outer structure. The inner structure is shown in a conventional contour map (Fig. 4); linear contour spacing is used, so that the faint halo structure does not show here.

The total flux in the CLEANed map is 6.28 Jy at 4885 MHz. Subtraction of a point source at the nucleus was employed to measure the core and jet fluxes. The core flux was 1.35 ± 0.05 Jy, with uncertainties due to lack of knowledge of the extended-component flux within ~0.″5 of the point source. The total jet flux was measured at $400(\pm 150)$ mJy, much in a dominant knot coincident with the optical knot but largely hidden by the core and restoring beam in Figures 3 and 4. The large uncertainty in this number mostly reflects possible differences in interpretation of extended emission as due to the jet or halo and in the structure of unrelated emission close to the nucleus.

The large-scale radio structure has several interesting properties. The emission is dominated by the core and a single lobe opposite the jet, with an elongated asymmetric halo, as shown in the intermediate-resolution map of Wardle, Moore, and Angel (1984). At the present resolution, much of the extended structure past the jet breaks up into blobs and filaments, with suggestions of asymmetry north-south. Particularly intriguing, if real, is the plume extending northward from the nucleus (Fig. 3). This feature has some of the apparent characteristics of a phase error in part of the data (especially in view of the "bay" south of the nucleus) and so warrants closer scrutiny. It appears at a level only $\sim 10^{-3}$ of the peak flux per beam, so the other map features discussed are more reliable.

Artifacts due to gross phase problems should have been reduced by the self-calibration procedure. No similar plume is seen near the more diffuse eastern lobe, so only high spatial frequencies could be involved. The feature's presence is relatively independent of the particular mapping procedure and restoring beam employed. Finally, an extension at this position is present in the Wardle, Moore, and Angel (1984) map. Confirmation of the existence of this feature would be highly desirable, since it might represent ejection at a position not related

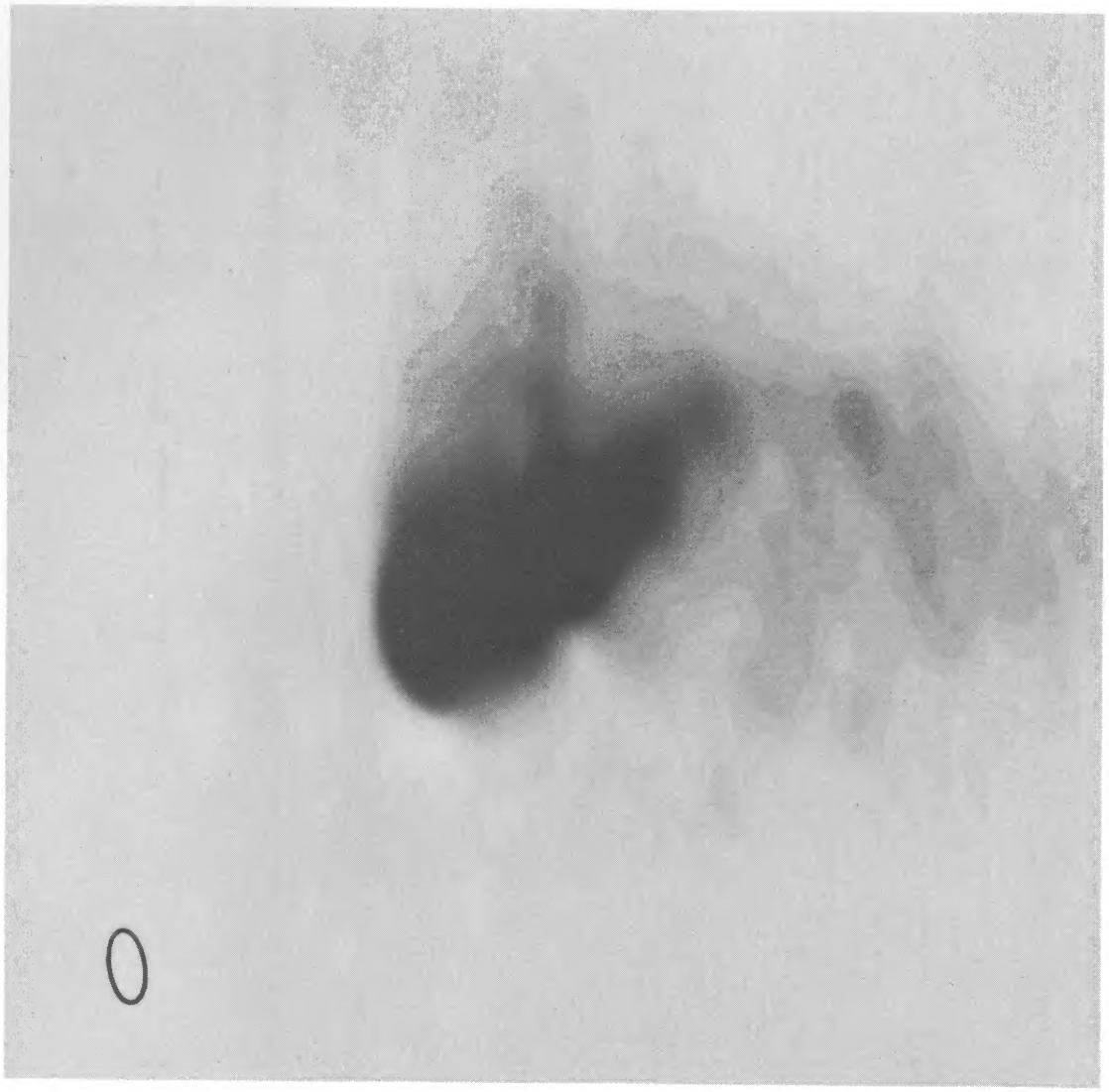

FIG. 3.—Gray-scale display of the 6 cm VLA B map of PKS 0521 − 36. The field is 60″ square, matching the area shown in Fig. 1. The map was restored after CLEANing with a Gaussian beam of half-power diameter 2″ × 4″ in P.A. 8°, shown by the ellipse. Note the asymmetric extended structure and curved extension of the jet.

KEEL (*see* page 298)

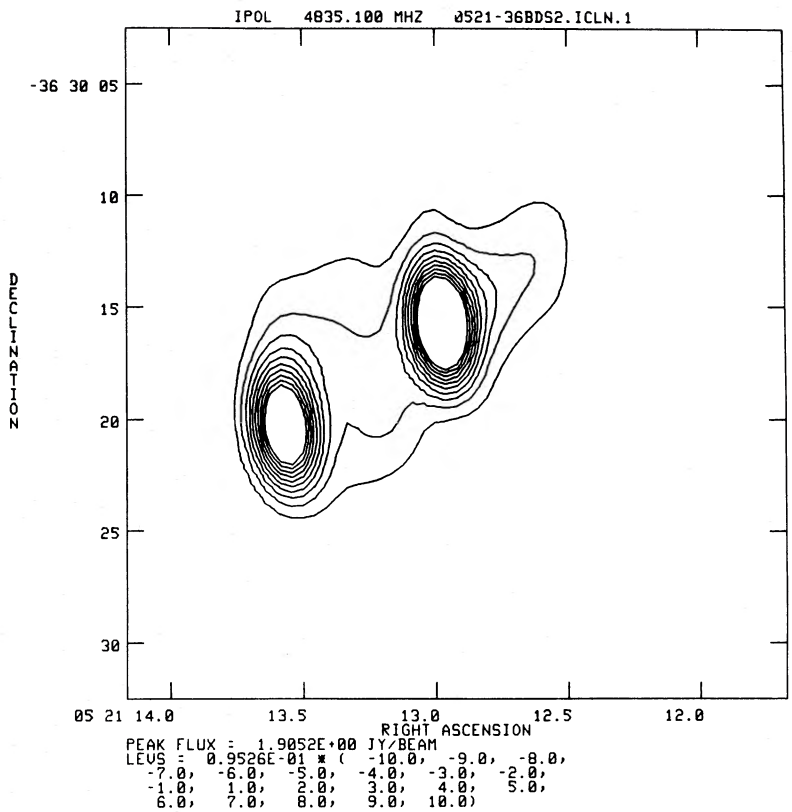

FIG. 4.—Contour representation of the inner region of PKS 0521−36 at 6 cm. Emission at the position of the brightest optical knot in the jet is visible on the west side of the central source.

to the jet or lobe. Alternately, it might be due to motion of the galaxy through a clumpy intergalactic medium, as envisioned by De Young, Condon, and Butcher (1980) for M87. However, the relatively severe sidelobes of the VLA at such southern declinations render interpretations of this feature based on available data premature and in any case not directly relevant to the jet structure.

The outer (large-scale) radio structure is rather similar to that of M87, as mapped by Turland (1975). Both show strong cores, jets, and asymmetric filamentary halos. The lobe in PKS 0521−36 is relatively brighter than that seen opposite the M87 jet, but similar structures appear in both cases.

The limitations of the 6 cm map and availability of higher resolution optical data warranted mapping at higher resolution. The core, jet, and southeast "hot spot" were mapped at 2 cm with the VLA in a hybrid array (north arm of the A configuration plus the rest of the B configuration), on 1985 March 31. For this observation, the object was observed over the entire range when it was above the array's elevation limit, again with frequent calibrator observation; these covered a large enough parallactic angle to allow polarization calibration. At 2 cm, Faraday rotation has been neglected. Atmospheric phase stability was quite poor at this high frequency and low elevation, so that self-calibration was essential. The core dominates sufficiently at 2 cm that a single iteration starting with a point-source model yielded a useful map, and further iterations produced no improvement. The hybrid array yielded a very circular beam; the central peak is well fitted by a Gaussian of $0''.30 \times 0''.31$ (FWHM), which was used in restoring the CLEANed maps.

The (u, v)-coverage was improved through an interleaving technique. The AC and BD correlator pairs were set to frequencies 350 MHz apart, so that, in the combined data set, gaps between antenna pairs at long spacings at each frequency are filled in by the other. Spectral index changes across the source do not contribute significantly to the map noise over such a small frequency range. (I am indebted to Frazer Owen and Tim Cornwell for advice on this procedure). Note that the absolute positioning of features in the 2 cm maps is uncertain by $\sim 1''.5$, due to use of an assumed core position in the self-calibration stage.

These data reveal striking characteristics of both the jet and the opposed hot spot. As seen in the overall total-intensity map (Fig. 5), the jet shows a prominent transverse feature, corresponding to the optically unresolved knot (§ III*a*); this is clearly extended perpendicular to the jet in a manner reminiscent of knot A in M87 (Biretta, Owen, and Hardee 1983).

The hot spot is clearly resolved, and elongated east-west. Emission appears to the north in a "trail." The hot spot is thus clearly more diffuse than the core, which is unresolved here. Its orientation is about 30° off the line toward the nucleus.

The polarization properties of the resolved structures are also of interest. The jet (Fig. 6) is significantly polarized, with the highest polarized flux in the resolved knot; the position angle in the knot is at $\sim 45°$ to the jet direction, so that if one of the usual orientations (parallel or perpendicular to the jet) is present, complex unresolved structure must be important. Flux and polarization measurements integrated over several areas of interest are listed in Table 3. The jet outside the prominent knot is an excellent example of a high-polarization jet with

TABLE 3

2 cm FLUX AND POLARIZATION MEASUREMENTS

Region	Flux (mJy)	P (%)	$\theta°$
Core	2372	1.70	111.2
Jet (all)	106	22.3	48.9
Knot	60	9.8	75.0
Jet without knot	46	40.4	40.8
Hot spot	57	10.9	129.8
Northeast hot spot	33	16.0	82.1
Emission north of hot spot	108	13.3	144.6

implied magnetic field alignment along the jet (the polarization angle of 40° is within 5° [2 σ] of being perpendicular to the jet). The knot has lower fractional polarization (10% vs. 40%), and shows some evidence of internal structure.

The hot spot (Fig. 7) shows the radial polarization vectors common to hot spots in extended doubles (Laing 1981, 1982; Pooley 1982). A discrete emission region just to the northeast (subsidiary hot spot?) may show complex polarization structure. The hot spot itself shows an S-shaped polarization (and projected field) configuration. The extended emission to the north is distinct in P.A. from, but similar in degree of polarization to, the hot spot proper; it is so extensive that its flux in the 2 cm map (likely to be an underestimate due to its large scale) is nearly twice that of the hot spot.

III. THE JET OF PKS 0521−36

a) Structure

The most detailed information in the jet structure comes from the 2 cm map. It appears marginally resolved in width using a 0.″3 beam (which projects to 0.3 kpc for $H_0 = 75$). The jet is detected at 2 cm and in the optical to a distance of 6.″5 (6.8 kpc) from the nucleus.

The strong knot located 1.″7 (1.8 kpc) from the nucleus is clearly resolved transverse to the jet, with FWHM $\approx$ 1.″0 in this direction. It contains substructure near the limit of these data; its profile is not well approximated by a set of similar ellipses. Both rotations with flux level and flattenings or subcondensation are present.

The most obvious comparison of this feature is with knot A in the M87 jet, which exhibits similar flaring in width and substructure on a spatial scale 8 times smaller, at a similar distance from the nucleus (Biretta, Owen, and Hardee 1983).

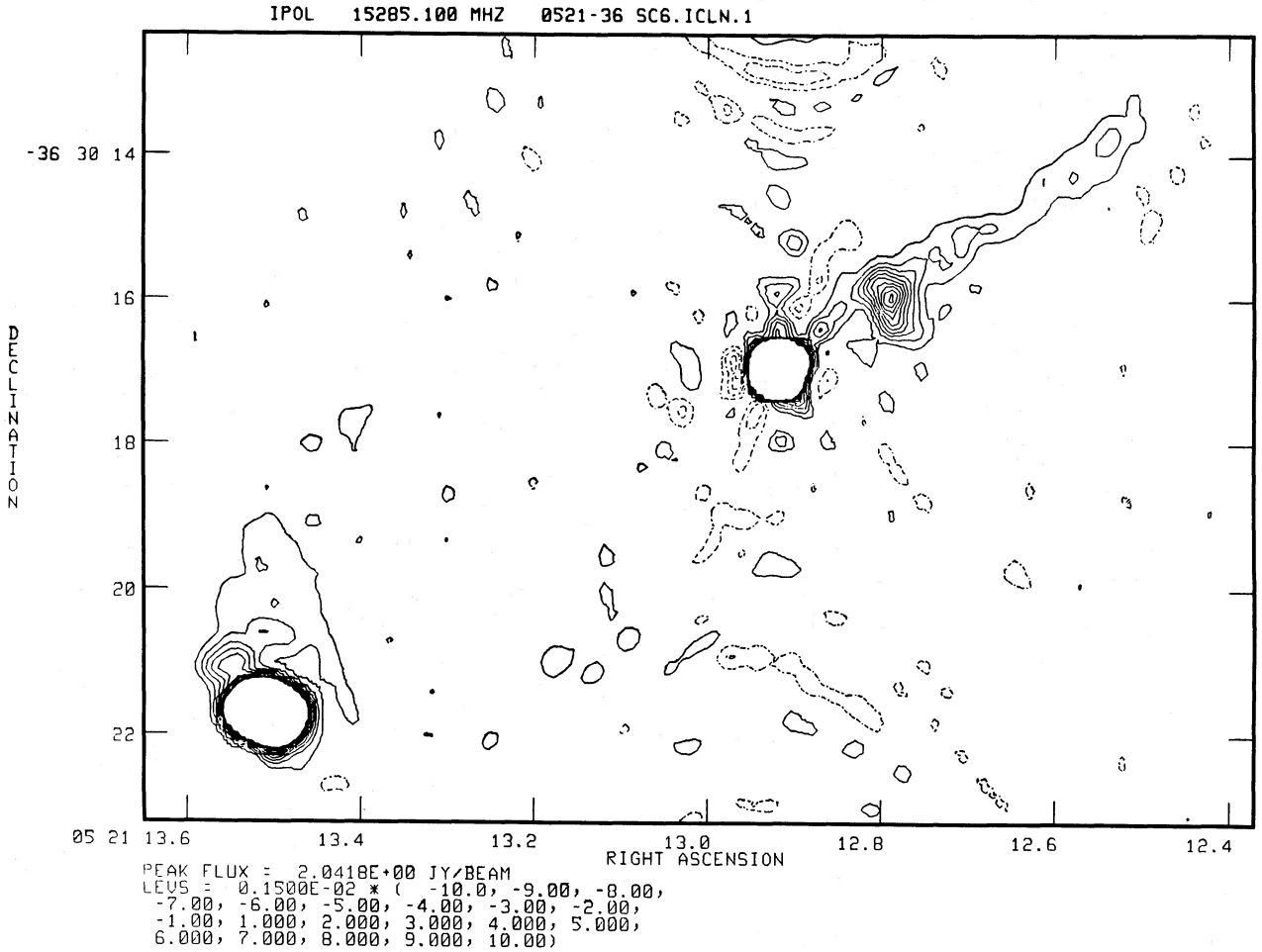

FIG. 5.—Total-intensity map of PKS 0521−36 at 2 cm, using the VLA in an A/B hybrid configuration. The beam is 0.″30 in diameter (FWHM). Note the transversely extended structure in the jet and opposing hot spot. Arcuate features north and south of the core are residual phase-closure artifacts. Absolute positioning is accurate only to ~1.″5.

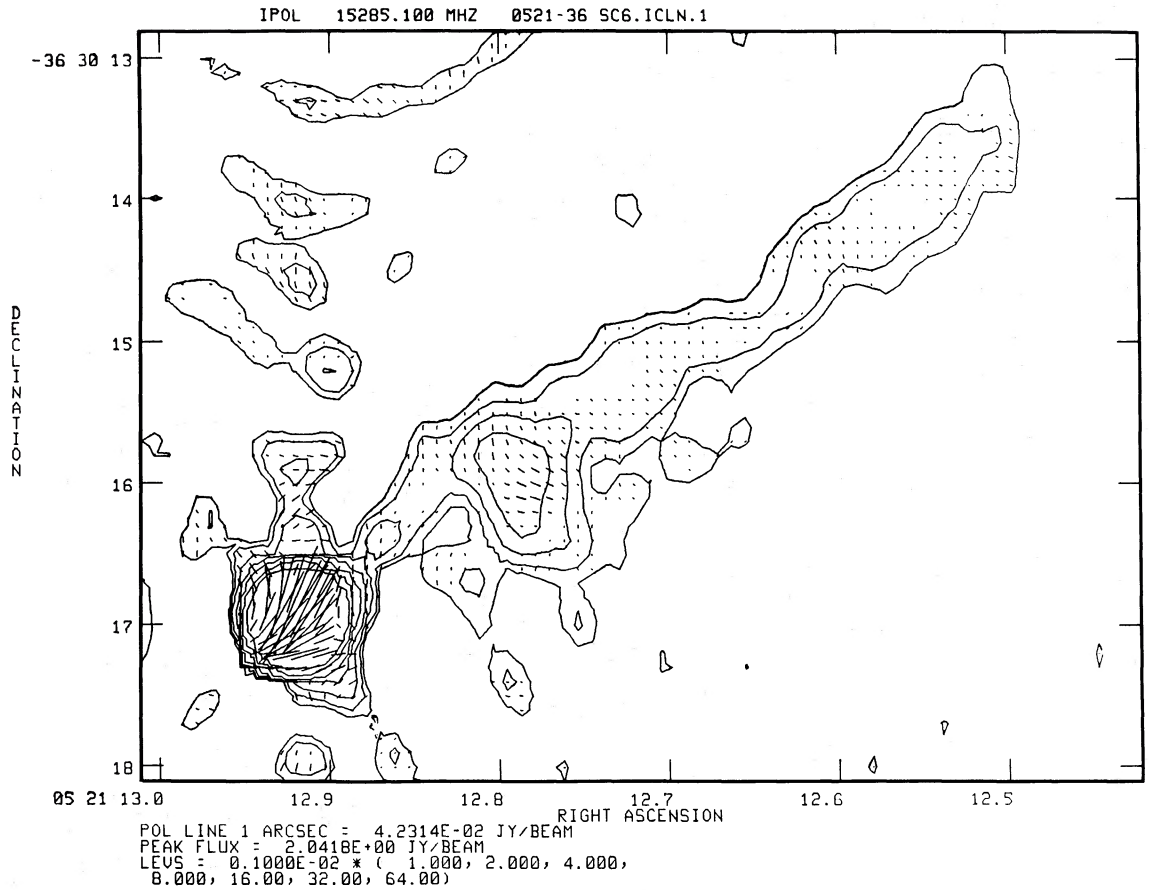

FIG. 6.—Contour map of the PKS 0521−36 jet at 2 cm, showing observed polarization vectors. Summing Stokes parameters in the jet (excluding the strong knot) confirms that the polarization is perpendicular to the jet; the knot itself has an integrated position angle of 75°.

They discuss the possibility that such features represent internal shocks, in which material in the inner part of the jet overtakes slower (decelerated?) jet matter. The widest part of the M87 jet occurs just outside knot A; no similar phenomenon would be seen in these data for PKS 0521−36, due to the short length of jet interior to the knot and confusion with low-level residuals this near the nucleus. There is some suggestion that the jet polarization interior to the knot is along the jet (Fig. 6); residual sidelobes severely compromise such a measurement within $\sim 1''$ of the core. A change from parallel to perpendicular senses is indeed seen at knot A in M87 (Owen, Hardee, and Bignell 1980).

The available resolution does not allow more detailed examination of the jet structure. In particular, the degree of clumpiness present in the M87 jet could be present and would be smeared into invisibility, as has been confirmed by convolving a representation of the M87 jet with various relevant beams. At this level, it can be said that its appearance is consistent with that of the M87 jet, if it were scaled to the same size and distance. The optical data on the 3C 31 and 3C 66B jets presented by Butcher, van Breugel, and Miley (1980) are consistent with similar degrees of dominance by discrete bright clumps. The other two objects with optical continuum and radio jets exhibit less clear connections; the synchrotron continuum in 3C 277.3 is confined to two knots (Miley *et al.* 1981), while the exact correspondence of optical and radio features in the 3C 273 jet is still unclear (e.g., Lelièvre *et al.* 1984).

b) Spectral Energy Distribution

Since available spectra indicate that the optical jet radiates mainly in the continuum, the photometric properties derived here may be used as indication of the slope of the spectrum. Galactic reddening at this position ($b = -35°$) is variously estimated at $A_B = 0.4$ (de Vaucouleurs, de Vaucouleurs, and Corwin 1976) and 0.16 (Sandage and Tammann 1981) for E_{B-V} of 0.10 and 0.04 respectively. With the observed $B-V = 0.65$ and the transformation of Sandage (1966), these give spectral indices $\alpha = -1.86$ and -2.11 respectively. The uncertainty due to photometric error exceeds that due to uncertain Galactic reddening, so I adopt $\alpha = -2.0 \pm 0.3$ integrated along the jet, with no measured gradient, which implies that any change in α_{BV} must be less than 0.2 over the jet. Comparison with the tapered 2 cm map, at the same resolution, shows a slight steepening of the 2 cm V spectrum with increasing distance from the nucleus (Fig. 8). The slope change is continuous along the jet, suggesting that it is not solely a difference between the inner knot and the jet proper.

Such a shift in optical-radio flux ratio might arise in at least two ways: change of the slope of all parts of the spectrum, or change in the turnover frequency. The radio-to-optical spectral index $\bar{\alpha}_{ro}$ integrated across the jet is 0.73; the optical index of 2.0 indicates that a strong break has occurred. The two slopes together suggest a break near 1 μm; this need only change by $\sim 40\%$ to produce the observed change in optical and radio flux profiles.

The presence of such a strong change in optical/radio flux contrasts strongly with the constant ratio (within a few percent) seen in M87 (Owen, Hardee, and Bignell 1980). This suggests that the acceleration of the highest energy particles in these objects occurs in different regimes.

The simplest way of interpreting the spectral data is to assume a single-component synchrotron form, as seems appropriate for M87. While not unique, such an interpretation provides a framework for comparison of various jets which is not contradicted by available data. In this case, the spectral data imply a lower frequency for a spectral break, and, given the steepness of the PKS 0521 − 36 jet spectrum in the optical, may indicate an exponential falloff. The flatter radio-to-optical index suggests that the change in spectral slope occurs not far redward of V. Infrared photometry would be valuable, since the jets' peak flux occurs somewhere in the near-IR, but will be difficult due to the faintness of the jet, strong galaxy background, and stronger nuclear radiation.

c) *The Red Tip*

A distinct knot off the jet tip appears in Figure 1 and the red photograph by Danziger *et al.* (1979). It is not present in the B image, implying $B-V > 1.5$. By this alone, it is clearly not simply a distant knot with properties similar to those of the inner jet.

Furthermore, this object does not have any 6 or 2 cm counterpart. Careful inspection of superposed V, 2 cm, and 6 cm images shows that the radio jet begins departing from a straight-line form closer to the nucleus than the reddish knot, and at this distance passes $\sim 1''.5$ to the north of the knot. If this object is actually associated with the jet (and not a background galaxy or foreground star), the closest analogy might be the emission regions at the edges of radio jets reported by Miley *et al.* (1981). However, failure to detect strong Hα at this position may mean that some continuum is also present. Because of the present spectrum's low sensitivity off the nucleus, especially in the red, this check should be repeated.

IV. A COMPARISON OF PKS 0521 − 36 AND M87

a) *Integrated Properties*

The similar host galaxies, radio properties, and possession of optical jets suggest that comparing these two objects in detail might prove useful in inferring the history and present state of activity of these systems. A number of parameters for PKS 0521 − 36 and M87 are listed in Table 4. M87 is taken to be at a

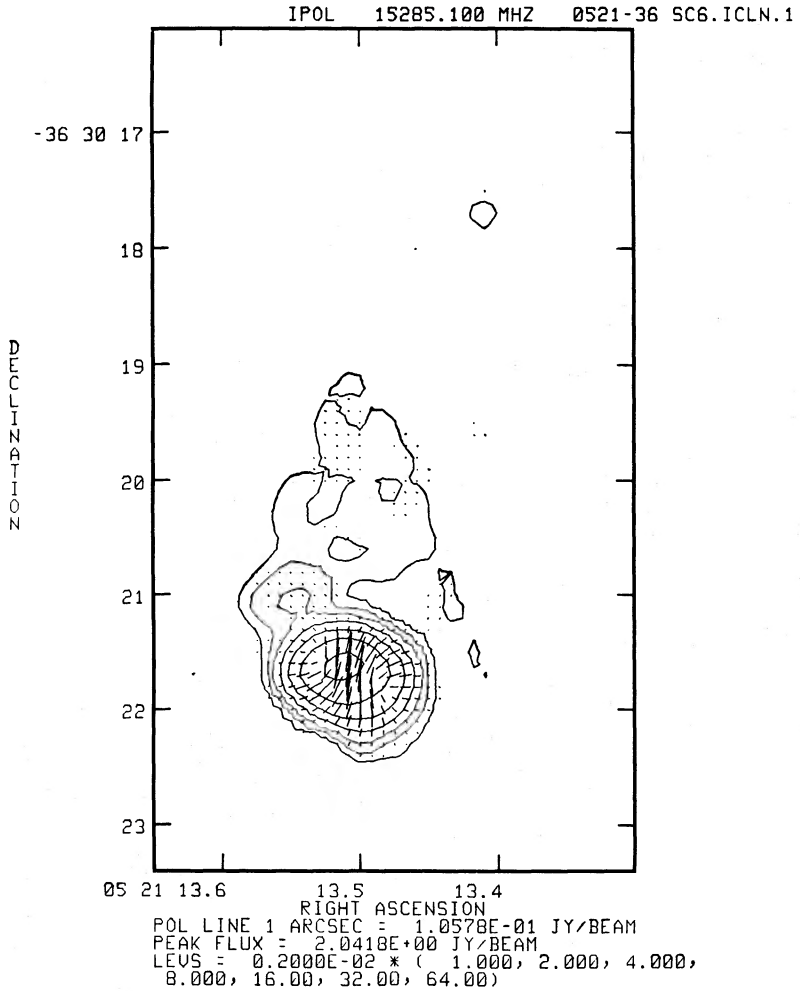

FIG. 7.—Contour map and polarization display of the PKS 0521 − 36 hot spot at 2 cm. The hot spot shows radial polarization vectors, with a central S-like configuration.

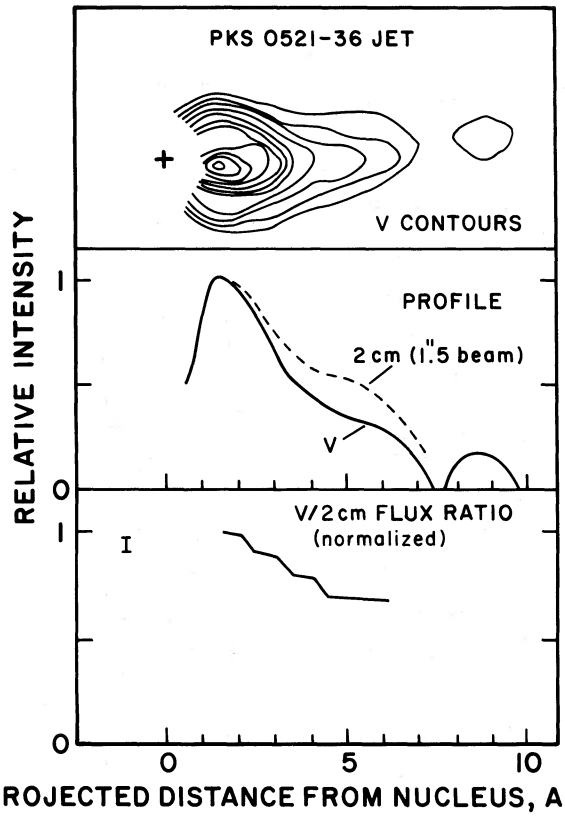

FIG. 8.—The intensity distribution along the jet of PKS 0521−36. (*top*) A contour map from the *V*-band CCD image; no optical data are shown within 1″ of the core source position, marked with a cross, due to increasing Poisson noise in the CCD data. (*middle*) *V*-band and 2 cm flux distribution along the jet, at matching resolution of 1″.5 FWHM. (*bottom*) the *V*/(2 cm) flux ratio as a function of position; a gradual, monotonic decrease with distance from the nucleus is seen. The ratio was evaluated in slices every 0″.5, so it has a choppy appearance in this figure.

distance of 20 Mpc, while $H_0 = 75$ km s^{-1} Mpc^{-1} is used for PKS 0521−36.

The host galaxies are very closely matched in absolute magnitude, though not in apparent ellipticity. PKS 0521−36 is 10 times as luminous at 1415 MHz as M87 (but 10 times as distant). The radio morphologies in the most extended structure are similar, with M87 about half as large to similar 6 cm surface brightness (using Fig. 2 of Turland 1975).

The most outstanding differences between these galaxies at a gross level are the presence of a strong radio hot spot opposite the jet in PKS 0521−36, and the much greater strength of its active nucleus, which can at times dominate the galaxy in the optical. By contrast, no optical nonthermal continuum has been clearly detected in the M87 nucleus. This difference cannot be solely a result of our seeing strongly beamed emission from the nucleus of PKS 0521−36, because its emission lines are much more luminous, and of much higher ionization, than in M87 (Table 4).

TABLE 4

ELLIPTICAL GALAXIES WITH CONTINUUM JETS

Parameter	M87	Reference	PKS 0521−36
Galaxy:			
M_B	−22.08	1	−22.33
L(1420 MHz) (ergs s^{-1} Hz^{-1})	5.9×10^{31}	2	7.8×10^{32}
Jet:			
Projected length (kpc)	2.1		10.9
M_B	−16.3		−16.7
α_{ro}	−0.66		−0.76
α_{opt}	−0.9		−2.0
L(15 GHz) (ergs s^{-1} Hz^{-1})	1.3×10^{30}		6.1×10^{30}
Nucleus:			
L(Hα) (ergs s^{-1})	3.3×10^{39}	3, 4	1.3×10^{41}
[O III] λ5007/Hβ	1.47		4.8

REFERENCES.—(1) Sandage and Tammann 1981. (2) Dixon 1970. (3) Heckman 1980. (4) Danziger *et al.* 1979.

There are somewhat contradictory arguments available regarding the extent to which the (optical and radio) core flux may be enhanced by beaming effects. The nucleus shows several properties placing it in the BL Lac or "blazar" class: strong optical variability (Eggen 1970), high optical polarization (~6%; Angel and Stockman 1980), and a flat-spectrum radio core. These objects may be understood with some success by a "unified scheme" (e.g., Scheuer and Readhead 1979), in which they are more normal radio galaxies viewed along a relativistic beam. In this instance, however, the visibility of a jet and hotspot suggest that we are not very close to the axis they define about the nucleus. For instance, the jet would be 50 kpc long if we are 10° from its axis; comparison of its physical properties with those of M87 (§ IV*b*) further suggests that the jet's radiation is not enhanced by any relativistic motion of the jet itself (in fact, the opposite). Since the core is not an extreme BL Lac object, these considerations may be resolved by moderate-angle (30°) beaming of the core in the same direction as the jet, preserving some enhancement through Doppler boosting while avoiding an unusually long (or intrinsically weak) jet.

It appears, in any case, that the different jet properties of M87 and PKS 0521−36 may be traced to their very different current states of nuclear activity. Some role might also be expected from the history of the nuclei and from the galaxies' somewhat different environments; these possibilities are elaborated below.

b) The Jets

Calculated properties of the jets are also included in Table 4. The PKS 0521−36 jet has not scaled up in radio or optical luminosity, or intensity per unit length, in step with the radio or nonthermal optical core luminosity as compared with M87. At the *V* band, the PKS 0521−36 jet is only twice as luminous as that in M87, while it has 4 times the projected length. The optical spectrum is redder than in M87, by $\Delta\alpha = 1.1$; the radio-optical slope is only slightly steeper.

Physical parameters of the jets may be compared if estimated in a consistent manner. Modeling each jet as a uniform cylinder (of diameter 100 pc for M87 and 300 pc for PKS 0521−36) and integrating the luminosity of each up to the (optical or infrared) turnover frequency, the equipartition magnetic fields are 10^{-4} and 5×10^{-5} G respectively; the lower value for PKS 0521−36 is derived mainly from its larger volume, so that if the jet is narrower than assumed here, the derived field will increase as (radius)$^{4/21}$. These figures are useful mostly for comparison; Owen, Hardee, and Bignell (1980) find fields ~3 times higher in knots A and B in M87. A global estimator was used here for more reliable comparison with PKS 0521−36.

Using spectral break frequencies of 1.0×10^{15} and 3.8×10^{14} Hz (and retaining a single-component model), these final values imply maximum electron energies of $\gamma = 9 \times 10^5$ (M87) and 7.6×10^5 (PKS 0521−36). These match to within the many uncertainties involved, and suggest that the difference in spectral shape between these jets is due mainly to a lower mean field in PKS 0521−36. The similar optical-to-radio spectra indices imply that the electron energy distribution is not greatly different between these objects. The cutoff frequency goes as the square of the maximum energy, so these measurements are very sensitive to this energy or to different average magnetic field values. The cutoff frequency ν_c is related to the highest particle energy (Lorentz factor γ) and local field B (in gauss) by

$$\nu_c \approx 1.76 \times 10^7 B\gamma^2 \sin\theta\,, \qquad (1)$$

where θ is the characteristic pitch angle. Geometric effects due to synchrotron pitch-angle distributions are probably not important, since at least in M87 the field is not *globally* ordered, from polarization measurements (Schmidt, Peterson, and Beaver 1978).

V. THE OCCURRENCE OF OPTICAL SYNCHROTRON JETS

Aside from M87 and PKS 0521−36, the only strong cases for active objects with kiloparsec-scale jets producing optical and radio synchrotron emission are 3C 31 and 3C 55B (Butcher, van Breugel, and Miley 1980). (While optical continuum has been seen from the jets of 3C 277.3 and 3C 273, these objects show morphological differences suggesting that additional processes are at work). In all these cases, the 5 GHz–5000 Å spectral index is in the range from −0.65 to −0.76; note that in even bright radio galaxies a slope of −0.75 or steeper would render the optical continuum undetected.

Clues to the distinct character of objects with optical jets may be found in their radio morphologies. All have strong cores, and high radio luminosities in the jets (the latter is a prerequisite for optical detection). Inspection of maps of 3C 31 (Fomalont *et al.* 1980) and 3C 66B (van Breugel and Jägers 1982) shows a possible connection among all these sources.

Each radio galaxy with an optical synchrotron jet has either a single radio jet or a very unequal jet/counterjet pair (peak intensity ratio >3). That is, no optical emission has yet been detected from equal pairs of the 3C 449 type. Careful examination of more galaxies of each kind will be of great interest, to see whether this pattern is genuine or an artifact of the number and kinds of sources located nearby.

PKS 0521−36 is unusual among these objects in showing two separate levels of asymmetry. The combination of a jet and hot spot on the opposite side is rare; another such case is 3C 200 (Burns 1984). Such systems appear to represent cases in which either one jet is essentially invisible (that feeding the hot spot), or in which the direction of outflow from the nucleus has just reversed, so that the visible hot spot is no longer being supplied by the nucleus and a new one has yet to be formed beyond the present jet. A population of such objects is expected in the "flip-flop" ejection picture (Rudnick and Edgar 1984), especially if the whole source is young or does not frequently flip, so that only one hotspot will be radiating while the jet begins going in the opposite direction.

Spectral shape measurements within the optical band are not yet available for the jets in 3C 31 or 3C 66B. They will be important in view of the different properties of M87 and PKS 0521−36 as regards optical slope, turnover frequency, and the spatial variations of these. Measures of all these objects in the 1–5 μm range will be useful in specifying the turnover frequency and detailed spectral shape. Any emerging systematics would lead to connection between the large-scale properties of these sources and the local physics of particle accelerates in the jets. Comparisons of M87 and PKS 0521−36 suggest such a connection, between the mean magnetic field and jet length (age?), but with only two objects studied, such physical conclusions are clearly premature. All the available optical synchrotron jets do suggest that electrons reach $\gamma \approx 10^6$ only in sources with somewhat asymmetric geometry.

There is one definite coincidence between the M87 and PKS 0521−36 jets that may bear on the interaction between the jets and their environments. The "flares" or internal shocks marking the brightest points in each occur at nearly the same projected distance from the nucleus in each case. Since the galaxies themselves are quite similar, this presumably implies similar local conditions, in particular pressure of the (mostly hot) interstellar medium. Sumi and Smarr (1984) have interpreted such structures as being due to encounters between jets and cooling flows in central galaxies of relatively rich clusters. The presence of such a feature at a similar location in PKS 0521−36 suggests a more complicated picture, or at least a more important role for the galaxies' own interstellar media. The environment of PKS 0521−36 is much sparser than the Virgo Cluster, and most of the extended emission-line structure seems to be related to the radio-emitting plasma, rather than to a cooling flow (Danziger *et al.* 1985). If a cooling flow is present, a moderately rich cluster is clearly not a prerequisite for its existence.

VI. CONCLUSION

New optical and radio data on the jet of PKS 0521−36 show it to resemble that of M87 in morphology. Its optical spectrum is notably steeper, probably implying a lower energy cutoff for the radiating electrons. The jet's optical-to-radio spectrum steepens by $\Delta\alpha \approx 0.07$ going outward along the jet, in an apparently continuous manner. This stands in contrast to the constant value reported in M87. In both objects, a significant flaring of the jet (internal shock?) occurs at a projected distance of ~ 2 kpc from the nucleus; given the similarity of galaxy properties, this might represent interaction between the jet and interstellar medium of each galaxy.

Comparison of known optical-radio synchrotron jets shows them to occur in one-sided or very asymmetric jets, suggesting that only in sources at an appropriate stage of development are electron energies up to $\gamma = 10^6$ reached.

I have benefited from conversation with Drs. Hélène Sol, Miller Goss, Peter Allan, Nigel Sharp, and Dave De Young. Srs. M. Hernandez, M. Navarrete, and R. Vanegas were most helpful and efficient at the telescope. Frazer Owen provided 2 cm flux measures of the M87 jet. The referee pointed out some bits of nonsense in an early version, which I hope have been eliminated.

REFERENCES

Angel, J. R. P., and Stockman, H. J. 1980, *Ann. Rev. Astr. Ap.*, **18**, 321.
Biretta, J. A., Owen, F. N., and Hardee, P. E. 1983, *Ap. J. (Letters)*, **274**, L27.
Burns, J. O. 1984, in *Physics of Energy Transport in Extragalactic Radio Sources*, ed. A. H. Bridle and J. A. Eilek (Green Bank: NRAO), p. 25.
Butcher, H. R., van Breugel, W. J. M., and Miley, G. K. 1980, *Ap. J.*, **235**, 749.
Danziger, I. J., Bergeron, J., Fosbury, R. A. E., Maraschi, L., Tanzi, E. D., and Treves, A. 1983*a*, *M.N.R.A.S.*, **203**, 565.
Danziger, I. J., Ekers, R. D., Goss, W. M., and Shaver, P. A. 1983*b*, in *Astrophysical Jets*, ed. A. Ferrari and A. G. Pacholczyk (Dordrecht: Reidel), p. 131.
Danziger, I. J., Fosbury, R. A. E., Goss, W. M., and Ekers, R. D. 1979, *M.N.R.A.S.*, **188**, 415.
Danziger, I. J., Shaver, P. A., Moorwood, A. F. M., Fosbury, R. A. E., Goss, W. M., and Ekers, R. D. 1985, *ESO Messenger*, **39**, 20.
de Vaucouleurs, G., de Vaucouleurs, A. and Corwin, H. G. 1976, *Second Reference Catalog of Bright Galaxies* (Austin: University of Texas Press).
De Young, D. S., Condon, J. J., and Butcher, H. R. 1980, *Ap. J.*, **242**, 511.
Dixon, R. S. 1970, *Ap. J. Suppl.*, **20**, 1.
Eggen, O. J. 1970, *Ap. J. (Letters)*, **159**, L95.
Fomalont, E. B., Bridle, A. H., Willis, A. G., and Perley, R. A. 1980, *Ap. J.*, **237**, 418.
Graham, J. A. 1982, *Pub. A.S.P.*, **94**, 244.
Heckman, T. M. 1980, *Astr. Ap.*, **87**, 152.
Keel, W. C. 1984, *Ap. J.*, **279**, 550.
Koski, A. T. 1978, *Ap. J.*, **223**, 56.
Laing, R. A. 1981, *M.N.R.A.S.*, **195**, 261.
Laing, R. A. 1982, in *IAU Symposium 97, Extragalactic Radio Sources*, ed. D. S. Heeschen and C. M. Wade (Dordrecht: Reidel), p. 161.
Lelièvre, G., Nieto, J.-L., Horville, D., Renard, L., and Servan, B. 1984, *Astr. Ap.*, **138**, 49.
Miley, G. K., Heckman, T. M., Butcher, H. R., and van Breugel, W. J. M. 1981, *Ap. J. (Letters)*, **247**, L5.
Owen, F. N., Hardee, P. E., and Bignell, R. C. 1980, *Ap. J. (Letters)*, **239**, L11.
Pooley, G. G. 1982, in *IAU Symposium 97, Extragalactic Radio Sources*, ed. D. S. Heeschen and C. M. Wade (Dordrecht: Reidel), p. 53.
Rudnick, L., and Edgar, B. K. 1984, *Ap. J.*, **279**, 74.
Sandage, A. R. 1966, *Ap. J.*, **146**, 13.
Sandage, A. R., and Tammann, G. 1981, *A Revised Shapley-Ames Catalog of Bright Galaxies* (Washington: Carnegie Institution).
Scheuer, P. A. G., and Readhead, A. C. S. 1979, *Nature*, **277**, 182.
Schmidt, G. D., Peterson, B. M., and Beaver, E. A. 1978, *Ap. J. (Letters)*, **220**, L31.
Schwab, F. 1980, *Proc. SPIE*, **231**, 18.
Sol, H. 1983, in *Astrophysical Jets*, ed. A. Ferrari and A. G. Pacholczyk (Dordrecht: Reidel), p. 135.
Sumi, D. M., and Smarr, L. L. 1984, in *Physics of Energy Transport in Extragalactic Radio Sources*, ed. A. H. Bridle and J. A. Eilek (Green Bank: NRAO), p. 168.
Turland, B. D. 1975, *M.N.R.A.S.*, **170**, 281.
Ulrich, M.-H. 1981, *Astr. Ap.*, **103**, L1.
van Breugel, W. J. M., and Jägers, W. 1982, *Astr. Ap. Suppl.*, **49**, 529.
Wardle, J. F. C., Moore, R. L., and Angel, J. R. P. 1984, *Ap. J.*, **279**, 93.

WILLIAM C. KEEL: Sterrewacht Leiden, Postbus 9513, 2300 RA Leiden, The Netherlands